Fizika Nizkikh Temperatur, 2000, v. 26, No 7, p. 658–663

Phonon-assisted anti-Stokes excitation of the fluorescence of Mn^{2+} ions in the $CsMnCl_3{\cdot}2H_2O$ crystal

V. V. Eremenko, V. I. Fomin, and V. S. Kurnosov

B. Verkin Institute for Low Temperature Physics and Engineering
National Academy of Sciences of the Ukraine, 47 Lenin Ave., 61164, Kharkov, Ukraine
E-mail: eremenko@ilt.kharkov.ua

Received January 28, 2000

We demonstrate that anti-Stokes excitation of Mn^{2+} ions in $CsMnCl_3{\cdot}2H_2O$ crystal is possible through multi-phonon addition to the energy of the photons of exciting light. The deficit dE between the energy of the Mn^{2+} $^4T_1$ exciton and the photon energy of the He–Ne laser used as the source of illumination is compensated by simultaneous annihilation of several thermally activated lattice phonons. The absence of two-photon activation of the fluorescence was verified by measurement of the dependence of the fluorescence intensity on the intensity of the exciting light, which appears linear at fixed energy mismatch dE.

PACS: **78.55.–m**

Introduction

It is well known that fluorescence is usually optically excited using a frequency of the pumping source above the frequency of the fluorescent electronic transition. The positive difference between the energy of the exciting photon and the energy of the electronic level is expended on the creation of phonons (or another quasiparticles), so the process is called Stokes. The situation becomes quite different in the case when the difference has negative sign. Thus the only way to excite the electronic level is to add enough energy to the photon. Such a process is called anti-Stokes excitation of fluorescence, because it is accompanied by the simultaneous annihilation of some quasiparticles (usually thermally created). A number of experiments on anti-Stokes fluorescence excitation are known, but all of them deal with rare-earth compounds (see, for example, [1,2]). In present paper we investigate the anti-Stokes fluorescence excitation in a Mn-containing compound.

Recently we observed the presence of $^4T_1$ fluorescence of the Mn^{2+} ion at close to room temperatures under the condition of irradiation of a $CsMnCl_3{\cdot}2H_2O$ single-crystal sample with a He–Ne laser. This phenomenon is quite surprising at first glance because the energy of the lowest excitonic level $^4T_1$ in this compound is about 17 064 cm^{-1} (at 1.8 K) [3], whereas the energy of the exciting light is 15 803 cm^{-1}, so the energy difference $dE = 1\ 261\ cm^{-1}$ is substantially higher than the sample temperature T.

$CsMnCl_3{\cdot}2H_2O$, or CMC, is strongly anisotropic due to its layered and chainlike crystal structure. The CMC structure is described by the orthorhombic space group $Pcca$ (D_{2h}^8) [4]. The unit cell contains four formula units and has the dimensions $a = 9.060$ Å, $b = 7.285$ Å, and $c = 11.455$ Å. The Mn^{2+} ions are arranged in chains along the a axis. Each Mn^{2+} ion is surrounded by a coordination octahedron consisting of four Cl^- ions and two O^{2-} ions. Two of the Cl^- ions are shared by adjacent octahedrons, while the other two belong to only one octahedron.

The strong anisotropy of various physical properties of CMC originates from its chainlike structure; for example, it is responsible for the quasi-one-dimensional character of the antiferromagnetic ordering of Mn^{2+} spins at low temperatures [5]. The vibrational spectra of CMC reflect its layered and chainlike structure also [6–8]. They contain extremely low-frequency optical excitations (30–50 cm^{-1}). The unit cell of CMC contains two chains which are symmetric one to another about the inversion. It was found earlier [6] that the Davidov

splitting of the vibrational modes of the crystal, in consequence of the above fact, is small, so the interaction between chains is weak.

Detailed studies of the Stokes fluorescence show that the dynamic behavior of the Mn^{2+} $^4T_1$ exciton reflects the reduced dimensionality [3,9–11]. The optical excitations in CMC are localized, and the energy migration at low temperatures is very slow [11]. The strong coupling of the exciton with an OH stretching vibration causes its efficient nonradiative relaxation and quenching of the fluorescence. This is apparent from the increase of the fluorescence lifetime, by more than an order of magnitude, when the H_2O in CMC is replaced by heavy water D_2O [10].

2. Experimental setup

CMC single crystals of good optical quality were grown from saturated solutions of $MnCl_2{\cdot}4H_2O$ and CsCl. The clearly distinguishable habit of the crystals used in our investigations allows one to easily cut oriented samples relative to the crystallographic directions for sample preparation. The samples have the form of a rectangular parallelepiped and were polished to optical quality.

The spectra were recorded using a JOBIN YVON U-1000 double monochromator with a cooled photomultiplier, photon-counting electronics, and digital data storage. In order to avoid the polarizing effect of the monochromator, a depolarization wedge was placed in front of the entrance slit. Polarized Raman scattering and fluorescence measurements were made using a right-angle scattering geometry. As sources of exciting light for the experiments we used a 0.5-mW He-Cd laser ($\lambda = 441.6$ nm) and a 40-mW He–Ne laser ($\lambda = 632.8$ nm). The sample was mounted in an optical cryostat for measurements in a wide temperature range. The temperature of a sample was measured to an accuracy of 1 K using a copper-constantan thermocouple. The recorded spectra were corrected for instrument's spectral response to represent the results in the form of the quantum yield.

3. Experimental results and discussion

The experimentally observed features are shown in Fig. 1, which exhibits the spectra for different temperatures, which look like narrow Stokes and anti-Stokes Raman lines on a broad background of a Gaussian-like shape. Evidence that the broad band is of a fluorescence nature was obtained by comparison with the spectra obtained in the irradiation of the sample at the shorter wavelength (441.6 nm) of the He–Cd laser at the same temperatures. The energy of the photons of this source is 22 645 cm^{-1}, which is about 5 580 cm^{-1} higher than the fluorescent electronic level of CMC, so we are then dealing with the usual process of fluorescence excitation. Figure 2 shows this comparison. A temperature-dependent scale factor is only used to fit these bands; these scale factors are subsequently used as the temperature dependence of the relative quantum yield of anti-Stokes excited fluorescence. To check the constancy of the experimental conditions during the experiments, we monitored whether the areas of some Raman lines conformed to the Bose law:

$$I_{\text{Stokes}} = I_0\{1 + [\exp(\hbar\omega/kT) - 1]^{-1}\},$$

where ω is the phonon frequency and T is the temperature. In the case of anti-Stokes excitation of the fluorescence with the He–Ne laser the most intense lattice phonons, with frequencies of about 75, 205, and 217 cm^{-1}, were used, whereas in the case of Stokes excitation (He–Cd laser) the very

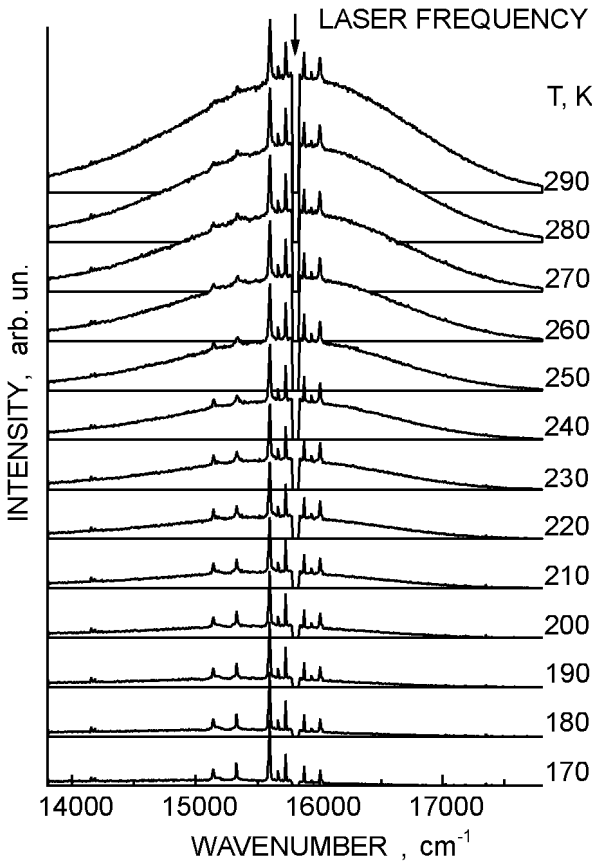

Fig. 1. Temperature dependence of the fluorescence overlapped with the Raman spectra excited by a He–Ne laser (15 803 cm^{-1}) in a $CsMnCl_3{\cdot}2H_2O$ single crystal. The fall in the spectra near the laser frequency is a result of shutting off the laser to prevent photomultiplier damage.

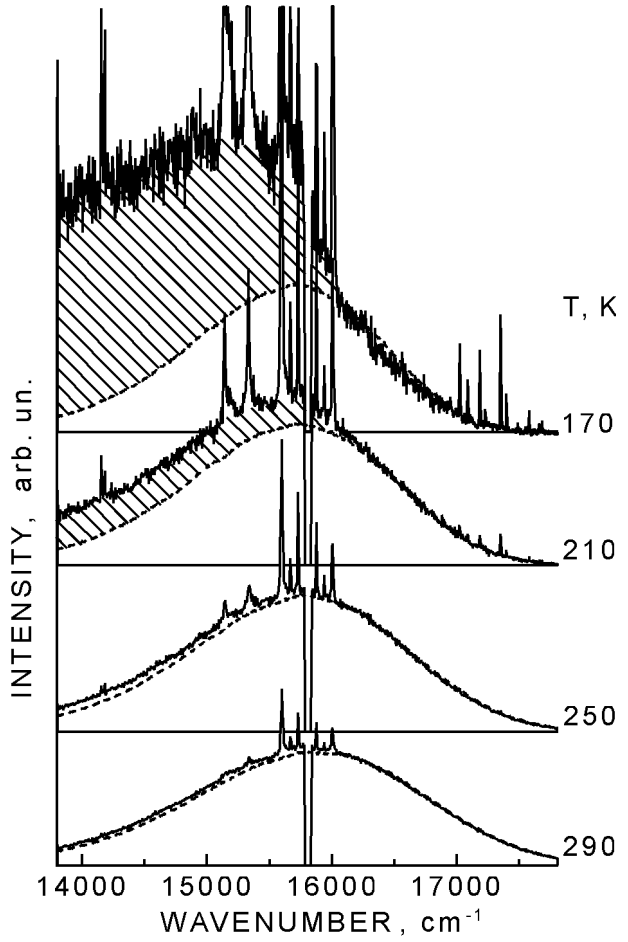

Fig. 2. Comparison of the fluorescence bands in a $CsMnCl_3{\cdot}2H_2O$ single crystal excited by He–Ne (solid lines) and He–Cd (dashed lines) lasers. The hatched areas represent the contribution of multi-phonon light scattering processes during excitation by a He–Ne laser.

intense phonon line at about 3 380 cm^{-1}, corresponding to an OH stretching vibration, was used.

At low temperatures the relative contribution of Stokes multiphonon light scattering increases, with an increasing scale factor, as shown in Fig. 2, giving the illusion of a difference between shapes, whereas at the highest temperatures the shapes match rather well. So, to calculate the relative factor of the efficiency of anti-Stokes excitation in comparison to the Stokes, at every temperature the high-energy slope of the fluorescence band was fitted. This slope corresponds to the anti-Stokes part of the Raman spectrum where the contribution of multiphonon scattering rapidly decreases with increasing Raman shift.

In order to check the mechanism of anti-Stokes excitation of the fluorescence, we measured the dependence of the emission intensity on the power of the He–Ne laser. It shows a linear dependence that excludes the possibility of multiphoton excitation.

Another exotic situation may give such a linear dependence, if one imagines that in the crystal there is some electronic level lower than Mn^{2+} $^4T_1$ and lower than the energy of a He–Ne laser photon. Such a level (of defects, for example) is conjectured to have a very long lifetime, so it is fully excited even at an extremely low density of irradiation. Thus the level may play the role of the initial level for a second step excitation of the Mn^{2+} $^4T_1$ electronic level. This scheme nevertheless does not stand up from the point of view of temperature dependence. Usually the lifetime of electronic excitations becomes longer with decreasing temperature, so the intensity of fluorescence must be at least nondecreasing, whereas the experiments display a contrasting behavior.

Polarization studies showed that the maximum intensity of the fluorescence band is observed with polarization along the direction of the chains, in the crystallographic direction a.

In order to check whether the experimentally observed temperature dependence of the quantum yield of the anti-Stokes excited fluorescence is consistent with the dependence of the absorption on the He–Ne laser wavelength, one needs to obtain the values of absorption coefficient. The main problem of such measurements is the very small value of the absorption. Another way is to calculate the anti-Stokes part of the absorption band using Stepanov's equation [12], which relates the shape of the fluorescence band with that of the absorption band, and vice versa. This expression has the form

$$\frac{I^{\mathrm{YIELD}}(\omega)}{\kappa(\omega)} \propto \omega^2 \exp\left(\frac{\hbar(\omega_0 - \omega)}{kT}\right),$$

where $I^{\mathrm{YIELD}}(\omega)$ is the quantum fluorescence yield at frequency ω; $\kappa(\omega)$ is the absorption coefficient at this frequency; and ω_0 is the frequency of the 0–0 electronic transition. Note that the expression has a universal character if the ground and excited states are in thermodynamic equilibrium and there are no alternative channels of absorption apart from the electronic transition. It is well known that phonons play an important role in processes of electronic absorption and radiation of light, so it is important to know the distribution functions of phonons in the electronic ground and excited states. We make the usual assumption that the initial phonon state is in thermal equilibrium with the medium and can be characterized by a Boltzmann distribution with an effective temperature T^*. In the case of optical absorption this is not an assumption but simply a

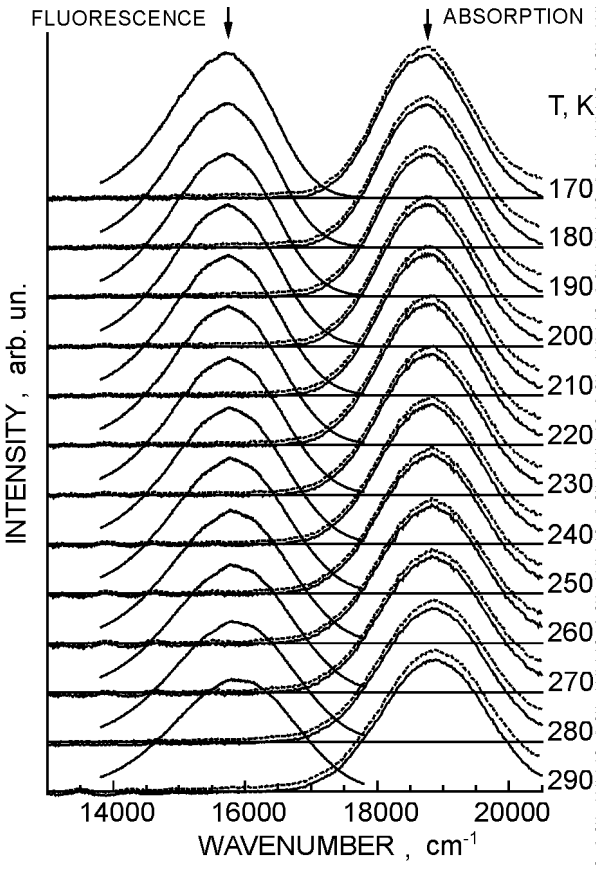

Fig. 3. Comparison of the fluorescence and absorption spectra of $CsMnCl_3{\cdot}2H_2O$ at different temperatures. The fluorescence was excited by a He–Cd laser (22 645 cm^{-1}). The solid absorption bands were obtained from the original ones (dashed bands) by subtracting the weak wing of the next absorption band with higher energy.

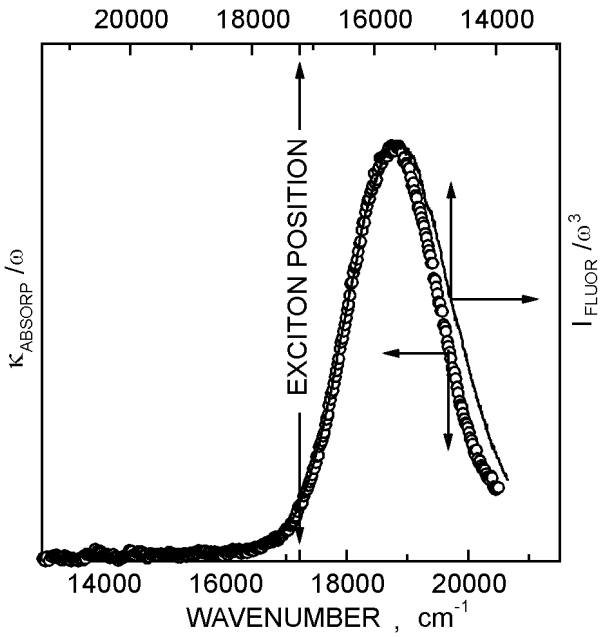

Fig. 4. Example of the fitting procedure for the determination of the pure exciton transition energy at a temperature of 230 K. The principle of «mirror» symmetry of the fluorescence and absorption renormalized line shapes is used. The slight difference between the bands is a result of the Franck – Condon interaction.

definition of the ground state with $T^* = T$. For the case which involves excited electronic states this assumption is valid subject to some conditions. It is known that the $^4T_1$ exciton in CMC has a long lifetime (0.58 ms in CMC with ordinary water and 9.2 ms in CMC with heavy water at $T = 1.8$ K [10]) in comparison with the lifetime of an optical phonon (usually 10^{-9}–10^{-11} s), so a close equality of T^* to the lattice temperature T can be justified also.

The absorption spectra were measured at the same temperatures as the fluorescence spectra, using samples of different thicknesses mounted in the two channels of the setup. This allowed us to ignore the light reflectance from the sample surfaces in the absorption coefficient calculations.

Thus, having experimental fluorescence and absorption spectra (see Fig. 3), it is possible to calculate the relative values of the absorption coefficient in the area of good transparency, if the frequency of the 0–0 electronic transition is known. The last problem may be solved also on the basis of the principle of so-called «mirror» symmetry of the fluorescence and absorption renormalized line shapes. The renormalization follows from the representation of the fluorescence yield and absorption coefficient in terms of the Einstein coefficients for spontaneous and stimulated electronic transitions. The renormalization has the form

$$\frac{I^{\mathrm{YIELD}}(\omega_0 - \Delta\omega)}{(\omega_0 - \Delta\omega)^3} \propto \frac{\kappa(\omega_0 + \Delta\omega)}{(\omega_0 + \Delta\omega)},$$

where $\Delta\omega$ is the relative frequency reccounted from the electron transition frequency ω_0. An example of such a fitting is presented in Fig. 4. The slight difference between the fluorescence and absorption bands is a result of Franck – Condon interaction, which in the present case may only slightly violate the principle presented above. Figure 5 represents the temperature dependence of the 0–0 electronic transition frequency obtained in present experiments together with the result of a direct observation at 1.8 K [3].

Using the results and methods presented above, the values of absorption coefficient at different temperatures were obtained. Examples of the use of Stepanov's law are shown in Fig. 6. A comparison of the directly observed areas of anti-Stokes excited fluorescence bands and the calculated absorption coefficients are in good agreement (Fig. 7).

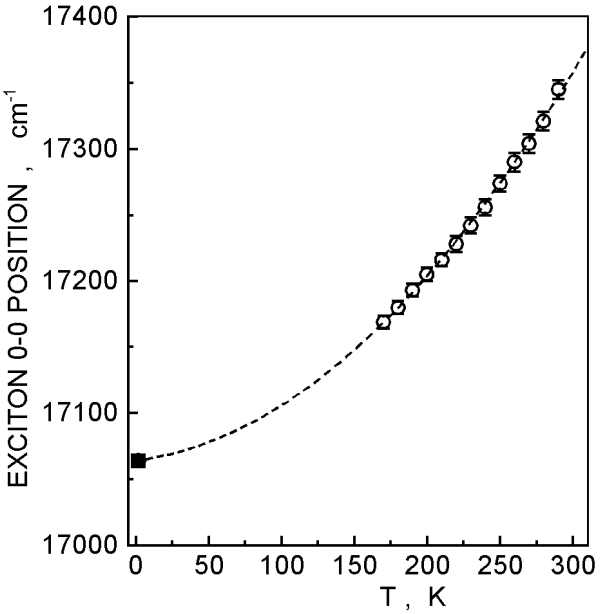

Fig. 5. Temperature dependence of the frequency of a pure excitonic transition in a $CsMnCl_3{\cdot}2H_2O$ single crystal. The open circles represent the exciton positions calculated in the present paper, whereas the solid square is the result of direct observation at 1.8 K [3]. The interpolated dashed line $\omega = \omega_0 + AT + BT^2$ is plotted using the following parameters: $\omega_0 = 17\ 064\ cm^{-1}$, $A = 0.139\ cm^{-1}/K$, $B = 0.0028\ cm^{-1}/K^2$.

It should be noted that the data obtained on the temperature dependence of the calculated absorption coefficient at the He–Ne laser wavelength and the corresponding experimental relative quantum yield of fluorescence conform well to the Arrhenius law (see Fig. 8). But the value obtained for the activation energy is not compatible with the real energy mismatches at all experimental temperatures. The cause of this illusion follows from a few accidental reasons. First of all, the position of the 0–0 excitonic level exhibits a temperature shift, as was shown above. In the temperature region of our experiments (170–290 K) the shift is close to linear (see Fig. 9). In addition, the position of the exciting wavelength at all temperatures remains near the maximum of the fluorescence band. Taking the above facts into account it is easier to understand the illusion. It follows from Stepanov's law that the absorption coefficient in the anti-Stokes region can be expressed in terms of the Stokes part of the fluorescence band as

$$\kappa(\omega) \propto \frac{I^{\mathrm{YIELD}}(\omega)}{\omega^2} \exp\left(\frac{-\hbar(\omega_0 - \omega)}{kT}\right).$$

Taking into account the approximately linear temperature dependence of $\omega_0 = \tilde{\omega}_0 + \alpha T$, one can obtain the following:

$$\kappa(\omega) \propto \frac{I^{\mathrm{YIELD}}(\omega)}{\omega^2} \exp\left(\frac{-\hbar(\tilde{\omega}_0 - \omega)}{kT}\right) \exp\left(\frac{-\hbar\alpha}{k}\right).$$

Because the Stokes-excited $I^{\mathrm{YIELD}}(\omega)$ depends hardly on the temperature at the frequency of the He–Ne laser (see Fig. 3), the Arrhenius law follows from the first exponent in the above expression, so the activation energy is simply the value $\hbar(\tilde{\omega}_0 - \omega_{\mathrm{laser}})$. If one uses the values given in the captions of Figs. 8 and 9 and a laser frequency $15\ 803\ cm^{-1}$, one sees easier that the values obtained are in very good agreement ($\tilde{\omega}_0 - \omega_{\mathrm{laser}} = 16\ 924 - 15\ 803 = 1\ 121\ cm^{-1} \approx \Delta E = 1\ 120\ cm^{-1} = 1615$ K).

Conclusion

The experiments and calculations presented show that the anti-Stokes excitation of fluorescence in CMC has a phonon-assisted character. The possibility of fluorescence excitation with a great energy

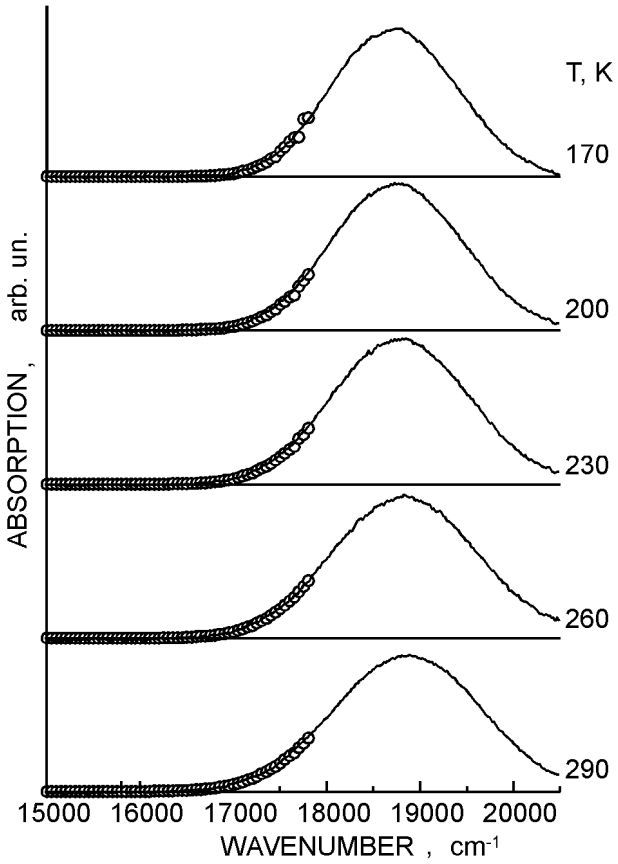

Fig. 6. Example of the fitting procedure for the determination of the weak absorption coefficient at the He–Ne laser frequency ($15\ 803\ cm^{-1}$) by comparison of the real absorption spectrum (solid line) with the part of the absorption band (open circles) calculated from the corresponding fluorescence band using Stepanov's equation.

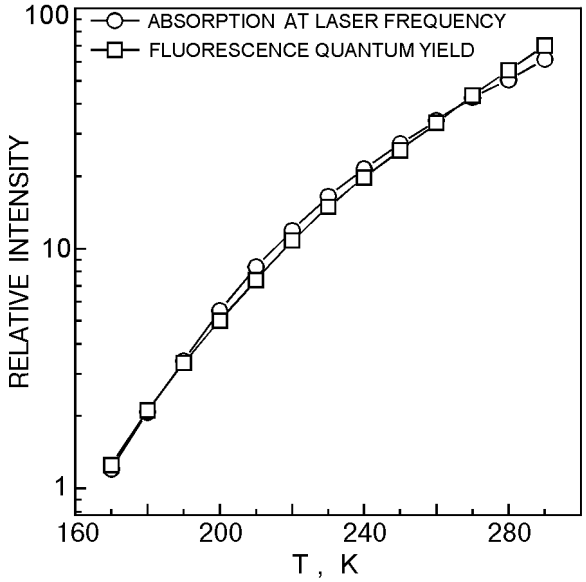

Fig. 7. Comparison of the data obtained for the absorption at the He–Ne laser frequency and the relative fluorescence quantum yield in a $CsMnCl_3{\cdot}2H_2O$ single crystal.

mismatch in comparison with the experimental temperatures seems likely to be a result of the chain-like crystal structure of $CsMnCl_3{\cdot}2H_2O$, which produces many low-frequency vibrational modes. These modes give a high phonon density of states in the low-energy region and are a cause of the well-developed absorption and fluorescence intensity in the immediate vicinity of the 0–0 electronic transition in both the Stokes and anti-Stokes regions. As a result of this work, the temperature dependence of the energy of the lowest level of the Mn^{2+} $^4T_1$ term in CMC was also obtained. It displays a very large

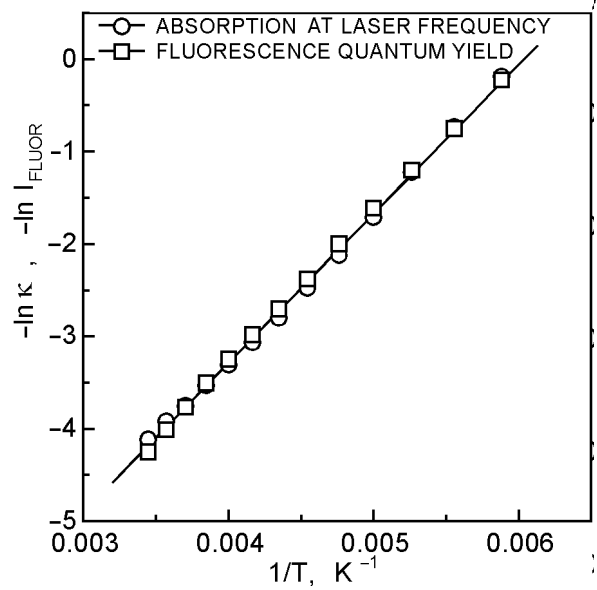

Fig. 8. Arrhenius temperature dependence of the relative absorption coefficient at the He–Ne laser frequency and the anti-Stokes excited fluorescence in a $CsMnCl_3{\cdot}2H_2O$ single crystal. The parameters of the interpolated line $y = y_0 + Bx$ are the following: $y_0 = -9.75$, $B = 1615$ K = 1 120 cm^{-1}.

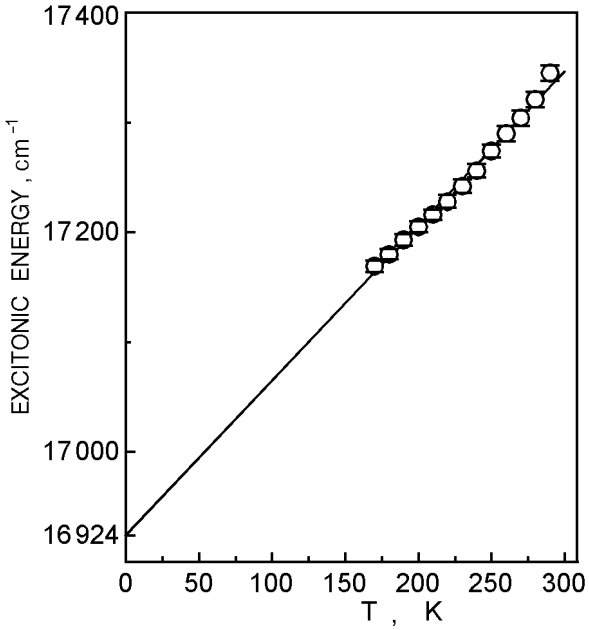

Fig. 9. Linear extrapolation of the experimentally determined temperature dependence of the 0–0 excitonic frequency in a $CsMnCl_3{\cdot}2H_2O$ single crystal.

temperature shift and reflects a large change in the crystal-field splitting of the level.

Acknowledgments

The authors would like to express their gratitude to I. S. Kachur for providing the CMC single crystals. We are thankful to professor D. Wolford and Dr. A. Frishman (both from Iowa State University) for the interest in this study and for helpful discussions. One of us (V.V.E.) thanks NATO for financial support (Grant PST. EV 975489).

1. F. Ausel, *Phys. Rev.* **B13**, 2809 (1976).
2. P. Raveendran, N. Sukar, and T. K. K. Srinivasan, *Phys. Rev.* **B55**, 4978 (1997).
3. W. Jia, E. Strauss, and W. M. Yen, *Phys. Rev.* **B23**, 6075 (1981).
4. S. J. Jensen, P. Anderson, and S. E. Rasmussen, *Acta Chem. Scand.* **16**, 1890 (1962).
5. K. Nagata and Y. Jazuke, *Phys. Lett.* **31A**, 293 (1970).
6. D. M. Adams and D. S. Newton, *J. Chem. Soc.* **A22**, 3499 (1971).
7. W. Jia, E. Strauss, W. M. Yen, K. Xia, and M. Zhao, *Phys. Rev.* **B39**, 12853 (1989).
8. V. P. Gnezdilov, V. V. Eremenko, V. S. Kurnosov, and V. I. Fomin, *Sov. J. Low Temp. Phys.* **17**, 331 (1991).
9. R. Ya. Bron, V. V. Eremenko, and E. V. Matyushkin, *Sov. J. Low Temp. Phys.* **5**, 344 (1979).
10. W. Jia, R. T. Brundate, and W. M. Yen, *Phys. Rev.* **B27**, 41 (1983).
11. V. V. Eremenko, V. A. Karachevtsev, A. R. Kazachkov, V. V. Shapiro, and V. V. Slavin, *Phys. Rev.* **B49**, 11799 (1994).
12. B. I. Stepanov, *Doklady Akademii Nauk SSSR* **112**, 839 (1957).